Dynamic structure function in ^{3}He-^{4}He mixtures

J. Boronat
Departament de Física i Enginyeria Nuclear, Universitat Politècnica de Catalunya, Pau Gargallo 5, E-08028 Barcelona, Spain

F. Dalfovo
Dipartimento di Fisica, Università di Trento, I-38050 Povo, Italy

F. Mazzanti and A. Polls
Departament d'Estructura i Constituents de la Matèria, Universitat de Barcelona, Diagonal 645, E-08028 Barcelona, Spain
(Received 4 March 1993)

Relevant features of the dynamic structure function $S(q,\omega)$ in ^{3}He-^{4}He mixtures at zero temperature are investigated starting from known properties of the ground state. Sum rules are used to fix rigorous constraints to the different contributions to $S(q,\omega)$, coming from ^{3}He and ^{4}He elementary excitations, as well as to explore the role of the cross term $S^{(3,4)}(q,\omega)$. Both the low-q (phonon-roton ^{4}He excitations and 1p-1h ^{3}He excitations) and high-q (deep-inelastic-scattering) ranges are discussed.

I. INTRODUCTION

From the theoretical viewpoint a dilute solution of ^{3}He in ^{4}He is a very appealing system since it is a mixture of fermions and bosons, having a small difference in mass and interacting via the same interatomic potential. In spite of the simplicity of this picture, the prediction of static and dynamic properties of ^{3}He-^{4}He mixtures is not at all simple and many problems are still open. Starting from the first idea that the ^{3}He atoms behave as a Fermi gas of quasiparticles,[1] several phenomenological theories have been proposed in the past, based on more or less refined effective interactions (see Ref. 2 for a review). The microscopic approach, based on *ab initio* calculations with a realistic interatomic potential, has proven quite hard. Recently, quantitative results for the ground state have been obtained by means of variational methods.[3,4] In Ref. 4, the ground-state properties of the mixture are calculated using the Aziz potential[5] and a Jastrow-type wave function, including also triplet correlations and summing up the elementary diagrams. The results for the radial distribution functions or, equivalently, for the static structure functions, clarify the role of the different kind of correlations in the system.

A complete microscopic theory for the dynamic properties of the mixture, based on the true many-body Hamiltonian, is still not available. The lack of such a theory is particularly unpleasant if one considers that accurate experimental data on the dynamic structure function $S(q,\omega)$ are now available, both at relatively low- ($0.5 < q < 2$ Å^{-1}) (Ref. 6) and high-momentum transfers.[7] On the other hand, it would be highly desirable to find a microscopic basis for different dynamical theories[8–11] based on various approximations for the linear response function, in terms of self-energy or pseudopotentials.

The aim of the present work is to take a first step in this direction. The main idea is to extract as much information as possible about $S(q,\omega)$, in the limit of zero temperature, using as input the ground-state calculations of Ref. 4. We make use of two different tools: the sum-rule formalism and the impulse approximation. The former is applied to separate and compare the different contributions to the dynamic structure function coming from ^{3}He and ^{4}He density excitations, as well as from the cross term $S^{(3,4)}(q,\omega)$. In particular, we analyze the moments m_0, m_1, and m_3, where

$$m_k(q) = \int d\omega\, (\hbar\omega)^k S(q,\omega)\ . \tag{1}$$

The sum rules contain useful information about the structure of $S(q,\omega)$ to be used both for the analysis of the experimental data and as a test of consistency for theoretical models. We will devote special attention to the relative weight of the density and spin-dependent dynamic structure functions of the ^{3}He component, as well as to the cross term $S^{(3,4)}(q,\omega)$; the role of the latter turns out to be non-negligible in a relevant range of q's. Finally, we will apply the sum-rule analysis to $S(q,\omega)$ in deep-inelastic scattering. The exact sum rules are compared with the results of the impulse approximation (IA), taking the momentum distribution from the calculations of Refs. 12 and 13.

II. SUM RULES

The sum-rule formalism has been extensively used in quantum many-body systems. A systematic review of sum rules for density and particle excitations in liquid ^{4}He is given by Stringari,[14] while recent calculations in ^{3}He are reported in Ref. 15. Sum rules in ^{3}He-^{4}He mixtures have been used in the past to explore the role of long-range correlations[16] and, more recently, to analyze neutron-scattering data.[6] In the following, we present the basic formalism and calculate sum rules for the different components of the dynamic structure function.

Let us introduce the definition of the density operators

$$\rho_{\mathbf{q}}^{(\alpha)} = \sum_{j=1}^{N_\alpha} e^{i\mathbf{q}\cdot\mathbf{r}_j}\ , \tag{2}$$

where $\alpha=3,4$ and N_α is the number of particles of α type. The dynamic structure function for density excitations at zero temperature is defined as

$$S^{(\alpha,\beta)}(q,\omega)=\frac{1}{2\sqrt{N_\alpha N_\beta}}\sum_n[\langle 0|\rho_q^{(\alpha)\dagger}|n\rangle\langle n|\rho_q^{(\beta)}|0\rangle+\langle 0|\rho_q^{(\beta)\dagger}|n\rangle\langle n|\rho_q^{(\alpha)}|0\rangle]\,\delta(\omega-\omega_{n0})\ . \tag{3}$$

For ^{3}He atoms one also introduces the spin density operator[17]

$$\mathbf{I}_q=\sum_{j=1}^{N_3}\mathbf{I}_j e^{i\mathbf{q}\cdot\mathbf{r}_j}\ , \tag{4}$$

where $\mathbf{I}_j$ is the spin of the j atom, and the spin-dependent dynamic structure function

$$S_I^{(3,3)}(q,\omega)=\frac{1}{N_3 I(I+1)}\sum_n|\langle n|\mathbf{I}_q|0\rangle|^2\delta(\omega-\omega_{n0})\ . \tag{5}$$

The total dynamic structure function is then[16,18]

$$\begin{aligned}S(q,\omega)=&\sigma_4(1-x)S^{(4,4)}(q,\omega)+\sigma_3 xS^{(3,3)}(q,\omega)\\&+\sigma_{3,I}xS_I^{(3,3)}(q,\omega)\\&+2\sigma_{34}\sqrt{x(1-x)}S^{(3,4)}(q,\omega)\ ,\end{aligned} \tag{6}$$

where $x=N_3/(N_3+N_4)$ is the ^{3}He concentration. Inclusion of the cross sections σ makes the quantity $S(q,\omega)$ directly proportional to the measured neutron-scattering cross section, with energy and wave-vector transfer $\hbar\omega$ and q. The values $\sigma_4=1.34$, $\sigma_3=4.42$, $\sigma_{3,I}=1.19$, and $\sigma_{34}=2.35$ (in units of b) are taken from Ref. 6.

Sum rules are rigorous relations among energy-weighted integrals of $S(q,\omega)$ and ground-state properties. The moments of the different components of $S(q,\omega)$ are defined in the following way:

$$m_{k,(I)}^{(\alpha,\beta)}(q)=\int d\omega\,(\hbar\omega)^k S_{(I)}^{(\alpha,\beta)}(q,\omega)\ . \tag{7}$$

Inserting the definitions of $S^{(\alpha,\beta)}(q,\omega)$ in Eq. (7), and using the completeness of the $|n\rangle$ states, one finds[19] that the moments m_k can be expressed as ground-state mean values of the density operator, the spin density operator, and the many-body Hamiltonian

$$\begin{aligned}H=&\sum_{j=1}^{N_3}\frac{-\hbar^2}{2M_3}\nabla_j^2+\sum_{j=N_3+1}^{N_3+N_4}\frac{-\hbar^2}{2M_4}\nabla_j^2\\&+\sum_{i<j}^{N_3+N_4}V(|\mathbf{r}_i-\mathbf{r}_j|)\ .\end{aligned} \tag{8}$$

Simple expressions can be written for the lowest k moments, as has already been done for pure ^{4}He and ^{3}He.[14,15] The main ingredients are the radial distribution functions and the kinetic energy per particle in the ground state. In the following, we discuss the m_0, m_1 and m_3 moments.

A. The m_0 moment

The m_0 moment of the dynamic structure functions is given by

$$\begin{aligned}m_0^{(\alpha,\beta)}(q)&=(N_\alpha N_\beta)^{-1/2}\langle 0|\rho_q^{(\alpha)\dagger}\rho_q^{(\beta)}|0\rangle\\&\equiv S^{(\alpha,\beta)}(q)\ ,\end{aligned} \tag{9}$$

where $S^{(\alpha,\beta)}(q)$ are the (α,β) components of the static structure function. The latter is related to the radial distribution functions $g^{(\alpha,\beta)}(r)$ through

$$S^{(\alpha,\beta)}(q)=\delta_{\alpha\beta}+\left[\frac{N_\alpha N_\beta}{\Omega^2}\right]^{1/2}\int d\mathbf{r}[g^{(\alpha,\beta)}(r)-1]e^{i\mathbf{q}\cdot\mathbf{r}}\ , \tag{10}$$

where Ω is the volume occupied by the system. For the spin-dependent component one has

$$m_{0,I}^{(3,3)}(q)=\frac{1}{N_3 I(I+1)}\langle 0|\mathbf{I}_q^\dagger\cdot\mathbf{I}_q|0\rangle\equiv S_I^{(3,3)}(q)\ , \tag{11}$$

where $S_I^{(3,3)}(q)$ is the spin-dependent static structure function. The latter can be written in terms of the spin radial distribution function

$$S_I^{(3,3)}(q)=1+\frac{N_3}{\Omega}\int d\mathbf{r}\,g_I^{(3,3)}(r)e^{i\mathbf{q}\cdot\mathbf{r}}\ , \tag{12}$$

where

$$g_I^{(3,3)}(r)=g_{\uparrow\uparrow}^{(3,3)}(r)-g_{\uparrow\downarrow}^{(3,3)}(r)\ . \tag{13}$$

In Eq. (13), $g_{\uparrow\uparrow}^{(3,3)}$ and $g_{\uparrow\downarrow}^{(3,3)}$ are the distribution functions for ^{3}He atoms having parallel and antiparallel spins, respectively, normalized in such a way that $g^{(3,3)}(r)=g_{\uparrow\uparrow}^{(3,3)}(r)+g_{\uparrow\downarrow}^{(3,3)}(r)$. All these quantities have been calculated in Ref. 4, where the concentration dependence of the static structure functions is discussed in detail. In Fig. 1, we show typical behavior of the m_0 moments at zero pressure and for two values of concentration. The static structure function associated with the

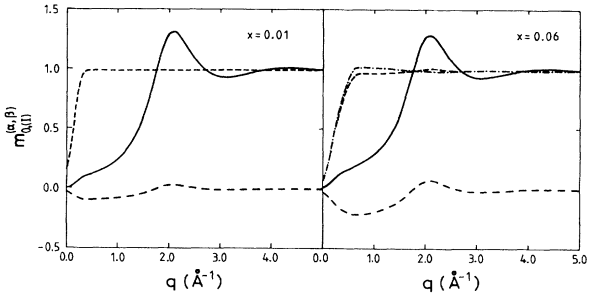

FIG. 1. The m_0 sum rules in the mixture at zero pressure and for two values of the ^{3}He concentration. Solid line, $m_0^{(4,4)}$; long-dashed line, $m_0^{(3,4)}$; short-dashed line, $m_0^{(3,3)}$; dot-dashed line, $m_0^{(3,3)I}$.

^{4}He component is nearly the same as in the pure ^{4}He phase. The ^{3}He component behaves almost as a gas of free fermions. Due to the weakness of spin correlations between ^{3}He atoms in the mixture, the spin-dependent moment is very close to the density moment, in particular, for $x=0.01$ it is indistinguishable. Finally, the moment m_0 of the cross term $S^{(3,4)}$ is significantly different from zero for q less than approximately 3 Å^{-1}. Its oscillating behavior reflects the fact that $S^{(3,4)}(q,\omega)$ is not positively defined.

B. The m_1 moment

The case of the m_1 moment is particularly simple. It corresponds to the energy-weighted sum rule, which can be expressed in the form of a double commutator, as follows:

$$m_1^{(\alpha,\beta)}(q)=\frac{1}{2(N_\alpha N_\beta)^{1/2}}\langle 0|[[\rho_{\mathbf{q}}^{(\alpha)\dagger},H],\rho_{\mathbf{q}}^{(\beta)}]|0\rangle \quad (14)$$

and

$$m_{1,I}^{(3,3)}(q)=\frac{1}{2N_3 I(I+1)}\langle 0|[[\mathbf{I}_{\mathbf{q}}^{\dagger},H],\mathbf{I}_{\mathbf{q}}]|0\rangle \ . \quad (15)$$

The commutators can be explicitly carried out, using the Hamiltonian (8), and the results are the well-known f sum rules:

$$m_1^{(4,4)}(q)=\frac{\hbar^2q^2}{2M_4} \ , \quad (16)$$

$$m_{1,I}^{(3,3)}(q)=m_1^{(3,3)}(q)=\frac{\hbar^2q^2}{2M_3} \ , \quad (17)$$

$$m_1^{(3,4)}(q)=0 \ . \quad (18)$$

The last result supplies a rather strong model-independent constraint to the cross term $S^{(3,4)}(q,\omega)$.

C. The m_3 moment

The generalization of the calculation of m_3 for the pure phase[14,15,20] to the case of ^{3}He-^{4}He mixtures is straightforward. Again, one has to evaluate commutators between $\rho_{\mathbf{q}}$, $\mathbf{I}_{\mathbf{q}}$, and H. The final results are

$$m_3^{(4,4)}(q)=\frac{\hbar^6q^6}{8M_4^3}+\frac{\hbar^4q^4}{M_4^2}t_4+\frac{\hbar^4\rho_4}{2M_4^2}\int d\mathbf{r}\,g^{(4,4)}(r)[1-\cos(\mathbf{q}\cdot\mathbf{r})](\mathbf{q}\cdot\nabla)^2V(r) \ , \quad (19a)$$

$$m_3^{(3,3)}(q)=\frac{\hbar^6q^6}{8M_3^3}+\frac{\hbar^4q^4}{M_3^2}t_3+\frac{\hbar^4\rho_3}{2M_3^2}\int d\mathbf{r}\,g^{(3,3)}(r)[1-\cos(\mathbf{q}\cdot\mathbf{r})](\mathbf{q}\cdot\nabla)^2V(r) \ , \quad (19b)$$

$$m_{3,I}^{(3,3)}(q)=\frac{\hbar^6q^6}{8M_3^3}+\frac{\hbar^4q^4}{M_3^2}t_3+\frac{\hbar^4\rho_3}{2M_3^2}\int d\mathbf{r}[g^{(3,3)}(r)-g_I^{(3,3)}(r)\cos(\mathbf{q}\cdot\mathbf{r})](\mathbf{q}\cdot\nabla)^2V(r) \ , \quad (19c)$$

$$m_3^{(3,4)}(q)=-\frac{\hbar^4(\rho_4\rho_3)^{1/2}}{2M_4M_3}\int d\mathbf{r}\,g^{(3,4)}(r)\cos(\mathbf{q}\cdot\mathbf{r})(\mathbf{q}\cdot\nabla)^2V(r) \ , \quad (19d)$$

where t_α and ρ_α are the kinetic energy per particle and the particle density of the α isotope, respectively. We calculate the moments (19a)–(19d) using the ground-state results of Ref. 4. In Fig. 2, we show the results for the m_3 moments of the ^{4}He and ^{3}He components at zero pressure and for $x=0.06$. The solid curves are the total moments (19a) and (19b), while the dashed lines are the corresponding potential part, i.e., the terms with the integrals of the interparticle potential $V(r)$ in the same equations. The spin-dependent moment (19c) is indistinguishable from the density moment (19b) on the scale considered. The oscillating behavior of the potential parts reflects the general structure of the radial distribution functions and the shape of the potential. The same holds for the cross moment (19d), which is plotted in Fig. 3.

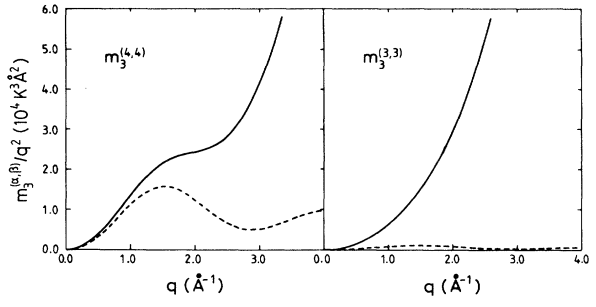

FIG. 2. The m_3 sum rules in the mixture at zero pressure and for $x=0.06$. Solid lines, sum rules $m_3^{(4,4)}$ and $m_3^{(3,3)}$, as in Eqs. (19a) and (19b); dashed lines, potential contribution to the same sum rules, i.e., the third term on the rhs of Eqs. (19a) and (19b). The spin-dependent sum rule $m_{3,I}^{(3,3)}$ is practically indistinguishable from $m_3^{(3,3)}$ on this scale.

III. DENSITY AND SPIN-DEPENDENT ^{3}He EXCITATIONS

First of all, we use the above sum rules to study the relative weight $m_k^{(3,3)}/m_{k,I}^{(3,3)}$ of the density and spin-dependent ^{3}He excitations. The case $k=0$ has been previously discussed in Sec. II A. The density and spin-dependent static structure functions are very close to each other, so that the ratio $(m_0^{(3,3)}/m_{0,I}^{(3,3)})$ is almost 1, even at low q. As is evident from Eq. (17), the ratio of the first moments is always equal to 1. Finally, the ratio $m_3^{(3,3)}/m_{3,I}^{(3,3)}$ at zero pressure and for two values of the concentration is plotted in Fig 4. When all the above ratios are close to 1, the effects of spin correlations on the dynamic structure function are negligible, and

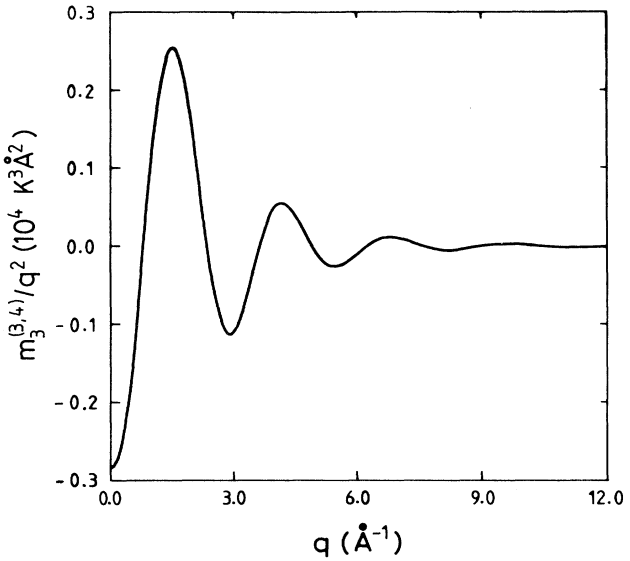

FIG. 3. The m_3 sum rule for the cross dynamic structure function in the mixture at zero pressure and $x=0.06$, as given in Eq. (19d).

$$S^{(3,3)}(q,\omega)\simeq S_I^{(3,3)}(q,\omega)\ . \tag{20}$$

This is certainly true for wave vectors much larger than the Fermi wave vector q_F. At $x=0.06$ the latter turns out to be 0.34 Å^{-1}. We note that for typical values of momentum transfer in neutron-scattering experiments one lies well above q_F, so that the difference between the density and spin-dependent structure functions can be safely neglected. As an example, we consider the values $q=1$ Å^{-1} and $x=0.045$, taken from a set of experimental values of Ref. 6. With these q and x we find

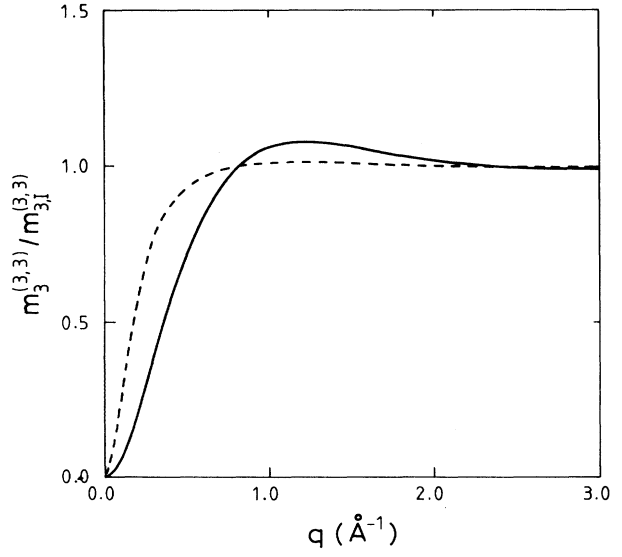

FIG. 4. Ratio between the contributions of density and spin excitations to the m_3 sum rule in the mixture at two different concentrations and at zero pressure. Solid line, $x=0.06$; dashed line, $x=0.01$.

$m_0/m_{0,I}=0.966$, $m_3/m_{3,I}=1.044$. These numbers give a microscopic basis to approximation (20) used in the analysis of the experimental spectrum.[6]

IV. THE CROSS TERM $S^{(3,4)}(q,\omega)$

The three sum rules (9), (18), and (19d) provide rigorous constraints to the cross term $S^{(3,4)}(q,\omega)$. From them it is easy to show how much $S^{(3,4)}(q,\omega)$ contributes to the moments of the total dynamic structure function. Let us take the four terms on the rhs of Eq. (6); one can calculate their $k=0$ and 3 moments (including σ factors and concentration) and divide them by the corresponding moments of the lhs. In Fig. 5, we show the results for $x=0.06$ and zero pressure. It appears that $S^{(3,4)}(q,\omega)$ gives a small contribution to the sum rules for q greater than approximately 3 Å^{-1}, while its contribution at lower q's is not at all negligible.

Let us focus our attention on the range $1<q<1.5$ Å^{-1}, where the neutron-scattering cross section shows two well-separated peaks, corresponding to ^{3}He and ^{4}He excitations.[6] A puzzling point in the experimental data is a strong quenching of the measured particle-hole peak of ^{3}He excitations with respect to a Fermi quasiparticle model. The data were analyzed with the assumption $S^{(3,4)}(q,\omega)=0$. Figure 5 shows that, in this range of q's, the contributions of the cross term to the m_0 and m_3 moments of the total dynamic structure function are comparable in magnitude with the ones of $S^{(3,3)}(q,\omega)$. In particular, $m_0^{(3,4)}$ is negative and $m_3^{(3,4)}$ is positive, while $m_1^{(3,4)}$ is zero. This fact suggests that $S^{(3,4)}(q,\omega)$ should be included in the analysis of the experimental spectrum. In principle, it is possible to satisfy the above m_k moments with a cross structure function distributed at high energies, with negligible contributions on the ^{3}He and ^{4}He peaks. This seems, however, quite unlikely. It is more reasonable to think that $S^{(3,4)}(q,\omega)$ should have a significant part of its strength in the region of ^{3}He and ^{4}He elementary excitations. To support this idea we suggest the following model.

Let us suppose that the total dynamic form factor is the sum of the following.

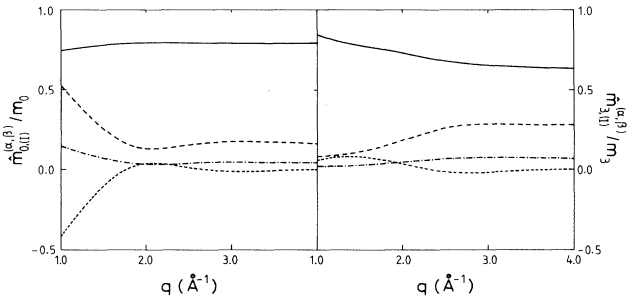

FIG. 5. Relative contributions of the different (α,β) components to the m_0 and m_3 moments of the total dynamic structure function in Eq. (6). The symbol $\hat{m}$ means that moments $m_k^{(\alpha,\beta)}$ have been multiplied by the corresponding σ and concentration factors. Solid line, (4,4); short-dashed line, (3,4); long-dashed line, (3,3); dot-dashed line, spin dependent (3,3). All curves correspond to zero pressure and concentration $x=0.06$.

(i) A peak centered around $\omega_{\text{p-h}}=\hbar^2q^2/2M_3^*$, where M_3^* is the effective mass of ^{3}He quasiparticles. The peak is the sum of $S^{(3,3)}(q,\omega)$ and $S^{(3,4)}(q,\omega)$. The latter is negative and follows approximately the shape of the ^{3}He peak.

(ii) A narrow peak at the frequency $\omega_0(q)$ of the phonon-roton branch, corresponding almost entirely to $S^{(4,4)}(q,\omega)$.

(iii) A band of multiparticle excitations above ω_0, corresponding to a broad distribution of strength coming mainly from $S^{(4,4)}(q,\omega)$ and partly from $S^{(3,3)}(q,\omega)$ and $S^{(3,4)}(q,\omega)$; the latter being positive and having the same broad distribution as the other two.

A qualitative sketch of the model is shown in Fig. 6. With these assumptions, and with approximation (20), it is possible to estimate how much strength the ^{3}He peak (p-h) takes from the $S^{(3,3)}$ and $S^{(3,4)}$ dynamic structure functions. A semiquantitative analysis is reported in Table I for $x=0.045$ and for two values of q. The first three rows are the exact moments calculated in Sec. II for the cross structure function. Due to the $(\hbar\omega)^3$ factor, the m_3 moment, as in pure ^{3}He and ^{4}He, is almost completely exhausted by multiparticle excitations. The ratios $\hbar\omega_{10}=m_1/m_0$ and $\hbar\omega_{31}=\sqrt{m_3/m_1}$ for multiparticle excitations are directly related to both the average energy and the broadness of multiparticle band. As an estimate of these ratios we take their values in pure ^{4}He at the same density,[21] since the general structure of the multiparticle band should not be changed dramatically by the presence of ^{3}He. With these numbers we calculate the multiparticle contributions to the moments $m_0^{(3,4)}$ and $m_1^{(3,4)}$. The difference between them and the total sum rules is an estimate of the strength in the region of the p-h peak. Now, let us define the dynamic structure function of the p-h peak as

$$S_{\text{p-h}}(q,\omega)=S_{\text{p-h}}^{(3,3)}(q,\omega)+\frac{2\sigma_{34}}{\sigma_3+\sigma_{3,I}}\left[\frac{1-x}{x}\right]^{1/2}S_{\text{p-h}}^{(3,4)}(q,\omega)\ . \quad (21)$$

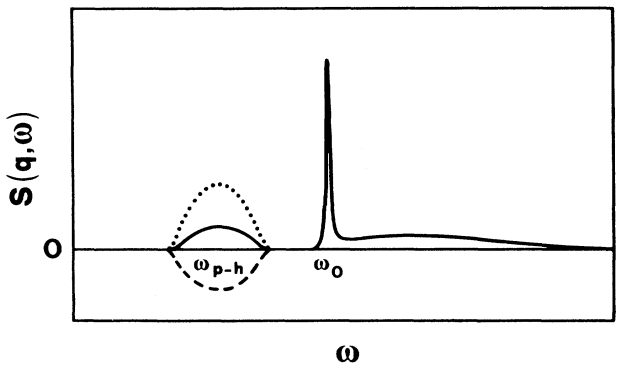

FIG. 6. Qualitative picture for the dynamic structure function in the range $q\simeq 1$–1.5 Å^{-1}. Solid line, total $S(q,\omega)$; dotted line, $S^{(3,3)}$ part of $S(q,\omega)$ in the particle-hole peak; dashed line, $S^{(3,4)}$ part in the same range. The different contributions to the multiparticle band are not shown. Scales are arbitrary. Only the proportions between the different contributions to the p-h peak are significant.

TABLE I. Quantities entering the analysis of Sec. IV, for $x=0.045$. First three rows: sum rules calculated in Sec. II. Rows 4 and 5: sum-rule ratios for multiparticle excitations, from estimates in pure ^{4}He (Ref. 21). Rows 6 and 7: m_0 and m_1 moments of $S^{(3,4)}(q,\omega)$ in the p-h range, estimated by subtracting the multiparticle part from the exact sum rules. Row 8: measured integrated strength of the p-h peak (from Fig. 11 of Ref. 6). Last two rows: results for the m_0 and m_1 moments of $S_{\text{p-h}}^{(3,3)}(q,\omega)$. See the text for a detailed discussion.

q (Å^{-1})	1.0	1.3
$m_0^{(3,4)}$	−0.160	−0.125
$m_1^{(3,4)}$ (K)	0	0
$m_3^{(3,4)}$ (K^3)	870	3320
$\hbar\omega_{31}$ (K)	60	65
$\hbar\omega_{10}$ (K)	35	35
$(m_0)_{\text{p-h}}^{(3,4)}$	−0.167	−0.148
$(m_1)_{\text{p-h}}^{(3,4)}$ (K)	−0.24	−0.79
$S_{\text{p-h}}(q)$	0.38	0.30
$(m_0)_{\text{p-h}}^{(3,3)}$	1.0	0.9
$(m_1)_{\text{p-h}}^{(3,3)}$ (K)	2.6	4.5

For a free Fermi gas $S_{\text{p-h}}(q,\omega)$ is a Lindhard function with integrated strength $S_{\text{p-h}}(q)=1$. The p-h peak has been measured in Ref. 6 and, through a Lindhard fit, results for the zero and first moments of $S_{\text{p-h}}$ have been given. From them, and from the microscopic results for the moments of the cross term, it is easy to obtain the moments of $S_{\text{p-h}}^{(3,3)}(q,\omega)$. The zero moment turns out to be almost 1 and the first moment is reduced by a factor $M_3^*/M_3\simeq 3$ with respect to the total f sum rule $\hbar^2q^2/(2M_3)$. Both results are consistent with the Fermi quasiparticle picture. The possible error in the last quantities due to the uncertainties in ω_{10} and ω_{31} is found to be of the order of 10%. Moreover, we have checked that, within the same accuracy, the results are concentration independent. The final outcome of this model is that the strength missing in the measured p-h peak can be associated with a negative cross term $S^{(3,4)}(q,\omega)$.

These results are consistent with the microscopic sum rules and with general physical arguments. Even if they should be considered qualitative rather than quantitative, they strongly support the importance of including the cross term in the theoretical investigation of the dynamic structure function. The role of the cross term was also studied by Lücke and Szprynger[10] in a random-phase-approximation- (RPA)- like scheme. In their theory $S^{(3,4)}(q,\omega)$ is relevant only when the ^{3}He quasiparticle peak and the ^{4}He phonon-roton peak are close and, eventually, overlap. In this case it produces an asymmetry of the roton peak, which, however, has not been observed. Our sum-rule analysis seems to justify the experimental findings; in fact, the contributions of the cross term to both the sum rules m_0 and m_3 in Fig. 5 are very small in

the region of overlap between the ^{3}He and ^{4}He excitations, changing sign near the roton wavelength ($q \simeq 2$ Å^{-1}).

V. $S(q,\omega)$ IN DEEP-INELASTIC SCATTERING

The density and spin-dependent dynamic structure functions, as defined in Eqs. (3) and (5), can always be decomposed in two pieces:[22–24]

$$S^{(\alpha,\beta)}(q,\omega)=S_c^{(\alpha,\beta)}(q,\omega)+S_{\rm inc}^{(\alpha,\beta)}(q,\omega) \ . \tag{22}$$

The first term is the coherent structure function and represents fluctuations which involve different atoms. The second term is the incoherent structure function (also known as self-correlation scattering function), which accounts for correlations between the position of the same atom at different times. One notes immediately that the cross term $S^{(3,4)}(q,\omega)$ is entirely coherent by definition. On the other hand, since the interatomic potential is spin independent, spin correlations between ^{3}He atoms arise only from symmetry properties of the many-body wave function; as a consequence, differences between the density and the spin-dependent structure functions for the ^{3}He component are restricted to their coherent parts, which for q not much larger than q_F become negligible.

The notation of coherent and incoherent scattering is useful in studying the dynamic structure function at high-momentum transfer. In fact, for sufficiently large q, the wavelength associated with the momentum transfer is small compared with the mean distance between the scattering atoms. In this limit, the piece of $S^{(\alpha,\beta)}(q,\omega)$ due to the interference of scattering amplitudes from different atoms is negligible and only the incoherent $S_{\rm inc}(q,\omega)$ will be left. Sum rules for the incoherent scattering can be easily evaluated; one has to carry out the same calculations of ground-state mean values as in Secs. II A–II C, but taking only the $i=j$ terms in the density and spin density operators. One finds[22–24]

$$m_{0,\rm inc}^{(\alpha,\alpha)}(q)=1 \ , \tag{23a}$$

$$m_{1,\rm inc}^{(\alpha,\alpha)}(q)=\frac{\hbar^2 q^2}{2M_\alpha} \ , \tag{23b}$$

and

$$m_{3,\rm inc}^{(\alpha,\alpha)}(q)=\frac{\hbar^6 q^6}{8M_\alpha^3}+\frac{\hbar^4 q^4}{M_\alpha^2}t_\alpha + \frac{\hbar^4 \rho_\alpha}{2M_\alpha^2}\int d\mathbf{r}\, g^{(\alpha,\alpha)}(r)(\mathbf{q}\cdot\nabla)^2 V(r) \ . \tag{23c}$$

Notice that $S_{\rm inc}^{(\alpha,\alpha)}$ saturates the total sum rule $m_1^{(\alpha,\alpha)}$ and therefore the coherent contribution to the f sum rule is zero.

Furthermore, one can generalize to the mixture the expansion of $S_{\rm inc}$ in inverse powers of the momentum transfer q, developed previously for pure phases.[22] The first term of this expansion is known as the impulse approximation. In the limit $q\to\infty$ the scattering simplifies considerably and only the first term (IA) survives. Then, the total $S(q,\omega)$ is given by

$$\lim_{q\to\infty} S(q,\omega)=S_{\rm IA}(q,\omega) =\sigma_4(1-x)S_{\rm IA}^{(4,4)}(q,\omega) +(\sigma_3+\sigma_{3,I})xS_{\rm IA}^{(3,3)}(q,\omega) \ , \tag{24}$$

where $S_{\rm IA}^{(\alpha,\alpha)}$ are directly related to the atomic momentum distributions $n_\alpha(k)$:

$$S_{\rm IA}^{(\alpha,\alpha)}(q,\omega) =\frac{\nu_\alpha \hbar}{(2\pi)^3\rho_\alpha}\int d\mathbf{k}\, n_\alpha(k)\delta\{\hbar\omega-[\epsilon(|\mathbf{q}+\mathbf{k}|)-\epsilon(k)]\} \ , \tag{25}$$

where $\mathbf{k}$ is the initial momentum of an α atom, $\mathbf{q}+\mathbf{k}$ is the final momentum of the recoiling α atom, and $\epsilon(k)=\hbar^2k^2/(2M_\alpha)$ is its kinetic energy. The δ function takes care of the conservation of energy in the scattering of a neutron from a single atom and ν_α stands for the spin degeneracy of each component ($\nu_4=1$, $\nu_3=2$).

To calculate $S_{\rm IA}^{(4,4)}$ one should take into account the macroscopic occupation of the zero-momentum state by ^{4}He atoms. To this end, it is convenient to write the momentum distribution of the different components in the following way:

$$n_\alpha(k)=\delta_{\alpha 4}(2\pi)^3\rho_4 n_0\delta(\mathbf{k})+\tilde{n}_\alpha(k) \ , \tag{26}$$

where n_0 is the condensate fraction of the ^{4}He component in the mixture, $\tilde{n}_4(k)$ stands for the occupation of the nonzero-momentum states of ^{4}He, and $\tilde{n}_3(k)$ is the whole momentum distribution of ^{3}He. In the following, we will write indistinctly $n_3(k)$ or $\tilde{n}_3(k)$. The momentum distributions $n_\alpha(k)$ defined in Eq. (26) are normalized in the following way:

$$\frac{\nu_\alpha}{(2\pi)^3\rho_\alpha}\int d\mathbf{k}\, n_\alpha(k)=1 \ . \tag{27}$$

Introducing expression (26) in Eq. (25) and performing the corresponding integrations one gets

$$S_{\rm IA}^{(4,4)}(q,\omega)=n_0\hbar\delta\left[\hbar\omega-\frac{\hbar^2q^2}{2M_4}\right] +\frac{M_4}{4\pi^2\rho_4\hbar q}\int_{k_4^{\rm min}}^{\infty} k\tilde{n}_4(k)dk \ , \tag{28a}$$

and

$$S_{\rm IA}^{(3,3)}(q,\omega)=\frac{M_3}{2\pi^2\rho_3\hbar q}\int_{k_3^{\rm min}}^{\infty} kn_3(k)dk \ , \tag{28b}$$

in which

$$k_\alpha^{\rm min}=\frac{M_\alpha}{\hbar^2 q}\left|\hbar\omega-\frac{\hbar^2q^2}{2M_\alpha}\right| \ . \tag{29}$$

Finally, one can also write the expressions for the first sum rules in the impulse approximation:

$$m^{(\alpha,\alpha)}_{0,\mathrm{IA}}(q)=1+\frac{\nu_\alpha}{4\pi^2\rho_\alpha}\int_{q/2}^{\infty}k\left[\frac{q}{2}-k\right]\tilde{n}_\alpha(k)dk\ , \tag{30a}$$

$$m^{(\alpha,\alpha)}_{1,\mathrm{IA}}(q)=\frac{\hbar^2q^2}{2M_\alpha}+\frac{\nu_\alpha\hbar^2q}{8\pi^2\rho_\alpha M_\alpha}\int_{q/2}^{\infty}k\left[\frac{q}{2}-k\right]^2\tilde{n}_\alpha dk\ , \tag{30b}$$

$$m^{(\alpha,\alpha)}_{2,\mathrm{IA}}(q)=\left[\frac{\hbar^2q^2}{2M_\alpha}\right]^2+\frac{4}{3}\frac{\hbar^2q^2}{2M_\alpha}t_\alpha+\frac{\nu_\alpha\hbar^4q^2}{12\pi^2\rho_\alpha M_\alpha^2}\int_{q/2}^{\infty}k\left[\frac{q}{2}-k\right]^3\tilde{n}_\alpha(k)dk\ , \tag{30c}$$

$$m^{(\alpha,\alpha)}_{3,\mathrm{IA}}(q)=\left[\frac{\hbar^2q^2}{2M_\alpha}\right]^3+\frac{\hbar^4q^4}{M_\alpha^2}t_\alpha+\frac{\nu_\alpha\hbar^6q^3}{16\pi^2\rho_\alpha M_\alpha^3}\int_{q/2}^{\infty}k\left[\frac{q}{2}-k\right]^4\tilde{n}_\alpha(k)dk\ . \tag{30d}$$

The main ingredients to calculate the impulse approximation are the momentum distribution of ^{4}He and ^{3}He atoms. They have been obtained in the (Fermi-)hypernetted-chain theory (HNC/FHNC) from a variational wave function containing two- and three-body correlations.[12,13]

First, we compare the exact sum rules, given in Sec. II, with the incoherent (23) and the impulse approximation (30) sum rules. We consider the case $x=0.06$ at zero pressure. In Fig. 7, we report the moment $m_0(q)$ for ^{3}He and ^{4}He excitations. While $m^{(4,4)}_{0,\mathrm{inc}}$ and $m^{(3,3)}_{0,\mathrm{inc}}$ are both equal to one, large differences appear between the total $m_0^{(3,3)}$ and $m_0^{(4,4)}$. This fact emphasizes the different behavior of the coherent contributions due to the different partial densities of both components. Since the ^{3}He density is very small, the coherent part of $m_0^{(3,3)}$ goes to zero faster than the one of $m_0^{(4,4)}$. Figure 8 shows the ratio of $m^{(3,3)}_{1,\mathrm{IA}}(q)$ to $m_1^{(3,3)}(q)$. As it has been mentioned before, $m_1^{(3,3)}$ is entirely incoherent, and $m^{(3,3)}_{1,\mathrm{IA}}$ reaches the asymptotic limit already at low values of q. The same conclusion applies to the ^{4}He component. Finally, we note that the m_3 sum rule, except in the $q\to0$ limit, is

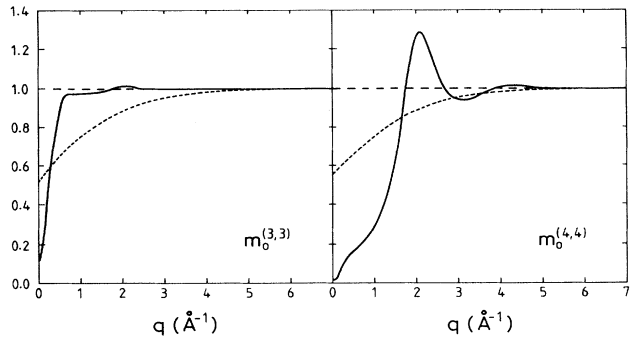

FIG. 7. Moments $m_0^{(\alpha,\alpha)}$ at $x=0.06$. Solid lines, static structure function; long-dashed lines, incoherent approximation; short-dashed lines, impulse approximation.

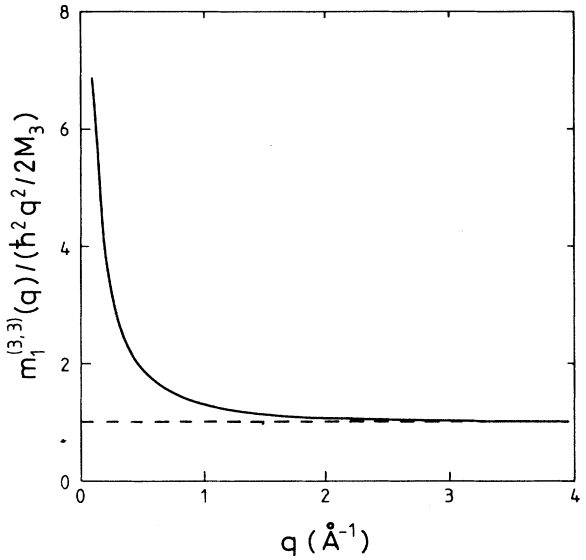

FIG. 8. Ratio between the moment $m_1^{(3,3)}$ and the f sum rule at $x=0.06$. Solid line, impulse approximation; dashed line, incoherent approximation.

dominated by its incoherent part. To prove this statement, the coherent contribution of m_3 for ^{4}He and ^{3}He excitations is shown in Fig. 9. The oscillations of $m_3^{(\alpha,\alpha)}(q)/q^2$ have a similar structure to the one of the total m_3 sum rule of the cross structure function $S^{(3,4)}(q,\omega)$. The results shown in Figs. 7–9 provide quantitative information about the quality of both the impulse and the incoherent approximations at a given q. Recent experiments of neutron scattering involve momentum transfer up to $q\simeq20$ Å^{-1} or even larger. In this range of q, the impulse approximation saturates all the sum rules considered here.

Second, we give explicit results for the dynamic struc-

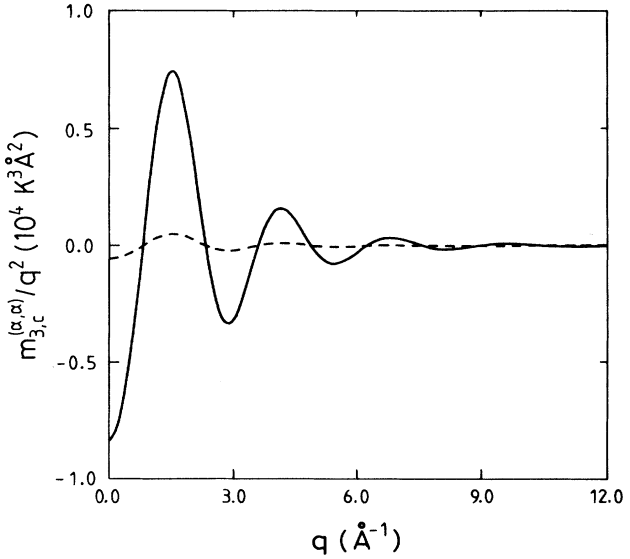

FIG. 9. Coherent part of the moments $m_3^{(\alpha,\alpha)}$ divided by q^2 at $x=0.06$. Solid line, $\alpha=4$; dashed line, $\alpha=3$.

ture function in impulse approximation. In Fig. 10, we show $S(q,\omega)$ calculated using Eq. (28) for two values of q (15 and 23 Å^{-1}), and for $x=0.06$. The deep-inelastic peak of each component is well distinguished and located at the recoiling energies of each component, i.e., $\hbar\omega_\alpha=\hbar^2q^2/(2M_\alpha)$. Notice that the δ contribution of the ^{4}He component [see Eq. (28a)] is not plotted in the figure. Due to its lighter mass, the peak of ^{3}He is located at a higher energy than that of ^{4}He, while for low-momentum transfer q the situation is just the opposite, so there should be a range of momenta where they closely overlap. The intensity of the ^{3}He peak is substantially smaller than the one of the ^{4}He because of the low ^{3}He concentration. Nevertheless, the difference is a little bit compensated by the fact that the ^{3}He cross section for the individual processes is four times larger than the ^{4}He one. In the IA, the height of the peaks decreases inversely proportional to q and the distance between them increases roughly as $\hbar^2q^2/6M_4$. On the other hand, they become wider making the overlap of the tails of the responses non-negligible.

The momentum distributions $n_4(k)$ and $n_3(k)$ have two important features. The former has the $k=0$ state occupied by a fraction of atoms n_0, which produces a δ peak in $S_{\rm IA}^{(4,4)}(q,\omega)$ at $\hbar\omega=\hbar^2q^2/2M_4$, not shown in Fig 10. On the other hand, $n_3(k)$ has a gap at k_F, which defines the strength of the quasiparticle pole Z_F at the Fermi surface and produces a discontinuity in the slope of $S_{\rm IA}^{(3,3)}(q,\omega)$ at $\hbar\omega=\hbar^2qk_F/M_3+\hbar^2q^2/2M_3$. However, these two features are actually smoothed out by both the experimental resolution[25] and the effects of the so-called final-state interactions (FSI).[24,26]

Although the experimental uncertainty in $S(q,\omega)$ makes a direct determination of the shape of $n_\alpha(k)$ rather difficult, one can still extract some averaged quantities. One of them is the kinetic energy per particle. In general, the experimental determination of the kinetic energy is based on the evaluation of the second energy moment of the response at q large enough so that only the incoherent part contributes. In that case one has

$$m_{2,\rm inc}^{(\alpha,\alpha)}(q)=\left[\frac{\hbar^2q^2}{2M_\alpha}\right]^2+\frac{4}{3}\frac{\hbar^2q^2}{2M_\alpha}t_\alpha\ . \tag{31}$$

Usually, a Gaussian centered at the recoiling energy is fitted to the experimental response and then one can analytically evaluate the kinetic energy. While this procedure gives results for pure ^{4}He,[25] in good agreement with sophisticated microscopic calculations,[27] large discrepancies appear in the case of pure ^{3}He.[25,28] The same problem appears in the analysis of the mixtures. In fact, preliminary experimental results[7] assign to the ^{3}He component a kinetic energy much lower than the theoretical predictions.[12,13] The latter can be derived either using the momentum distributions $n_\alpha(k)$ or evaluating the expectation value of the kinetic-energy operator in the trial variational wave function used to describe the mixture. For $x=0.06$ and zero pressure the theoretical values are approximately 19 and 14 K for ^{3}He and ^{4}He atoms, respectively. The ^{4}He kinetic energy is almost the same as in pure liquid ^{4}He. This follows simply from the fact that the density of the mixture is only slightly smaller than the saturation density of pure liquid ^{4}He. The microscopic calculation of pure ^{3}He at the saturation density predicts a kinetic energy around 13 K.[28] The increment in the kinetic energy of the ^{3}He component in the mixture with respect to the pure phase is due to the fact that the total density of the mixture is larger than the pure ^{3}He saturation density. Therefore, due to the correlations with the ^{4}He atoms, there are more ^{3}He atoms promoted above the Fermi surface.

We clarify this point in the context of the impulse approximation. The mean kinetic energy per ^{3}He atom t_3 can be explicitly calculated, using the momentum distribution $n_3(k)$, either by means of a direct integration

$$t_3=\frac{\nu_3}{(2\pi)^3\rho_3}\int d\mathbf{k}\frac{\hbar^2k^2}{2M_3}n_3(k)\ , \tag{32}$$

or through the definition of $S_{\rm IA}^{(3,3)}(q,\omega)$, as

$$t_3=\frac{3M_\alpha}{q^2}\int_{\omega_3}^{\infty}d\omega(\omega-\omega_3)^2S_{\rm IA}^{(3,3)}(q,\omega)\ , \tag{33}$$

where $\hbar\omega_3=\hbar^2q^2/(2M_3)$. The last equation is valid for any momentum transfer, but it is useful from the experimental point of view only at q large enough so that $S_{\rm IA}^{(3,3)}\sim S^{(3,3)}$. On the other hand, when $q\to\infty$ this way to calculate the kinetic energy is equivalent to the evaluation of $m_{2,\rm inc}^{(3,3)}$, as given in Eq. (31). In order to show the importance of the high-energy tail, we report in Fig. 11 the length of the energy interval, as a function of q, where the integration in Eq. (33) should be performed to get 50 and 95 % of the total t_3. For the sake of comparison, it is also plotted the length of the energy interval needed to integrate the response of the underlying free Fermi sea (a gas of fermions having the same q_F as ^{3}He atoms in the mixture) to get its total kinetic energy. The integration interval grows almost linearly with the momentum

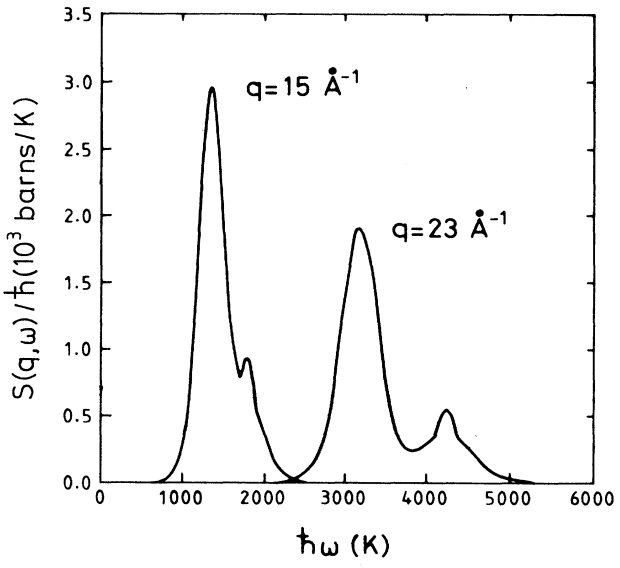

FIG. 10. Dynamic structure function in the impulse approximation for two values of q at zero pressure and $x=0.0$.

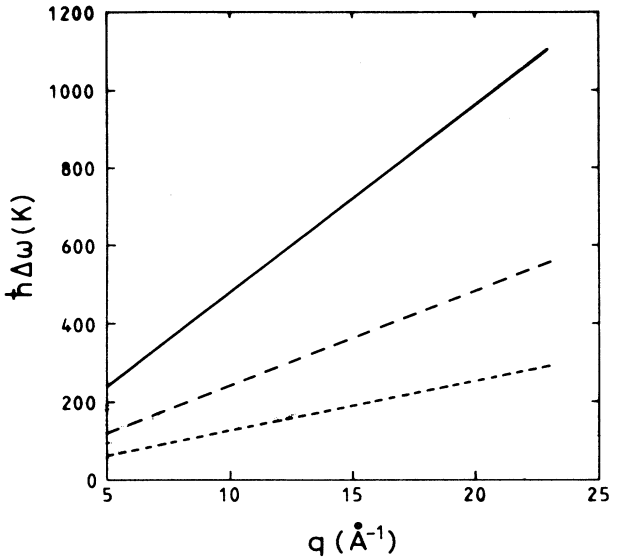

FIG. 11. Length of the energy interval in Eq. (33) needed to get 95% (solid line) and 50% (long-dashed line) of the mean kinetic energy t_3 as given in Eq. (32). Short-dashed line, free Fermi gas.

transfer. The slope of the line increases with the percentage of the kinetic energy required. In the case of the Fermi gas, the interval goes linearly with q with a well-defined slope: $\hbar^2 q_F/M_3$. Thereby, one needs to reach high momenta in order for the IA to be valid but, at the same time, the energy region where it is necessary to know the response increases with the momentum transfer. Our results, based on a microscopic calculation of the momentum distribution, reveal the role of the high-energy tail of the ^{3}He inelastic peak in determining t_3. Similar conclusions are obtained for the ^{4}He component but, in this case, the Gaussian fit to the deep-inelastic peak leads to a kinetic energy in good agreement with the microscopic calculations. This indicates that the Gaussian fit can account approximately for the wings of $S(q,\omega)$. Obviously, this fit is a better approximation for ^{4}He than for ^{3}He. The reason is that the underlying momentum distribution implied by a Gaussian $S^{(\alpha,\alpha)}$ is also of Gaussian type and it is clear that this shape of the momentum distribution reproduces $n_4(k)$ better than $n_3(k)$. It is also possible to appreciate, by a simple inspection of Fig. 10, that due to the discontinuity in the slope of $S^{(3,3)}$ it is more difficult to fit a Gaussian to the response of the ^{3}He component. In any case, to compare theory and experiments one also has to take into account FSI effects, which can change significantly the structure of the tail and smooth out the discontinuity in the slope at the Fermi surface, even at large q.

VI. CONCLUSIONS

In this work we have used the sum-rule formalism to investigate properties of the dynamic structure function in ^{3}He-^{4}He mixtures at zero temperature. The relevant quantities entering the sum rules have been taken from recent calculations of the ground state, based on variational wave functions with two- and three-body correlations.[4,12,13] We have discussed the m_0, m_1, and m_3 moments of the dynamic structure function, separating the different contributions coming from the ^{3}He and ^{4}He components, as well as from the cross term $S^{(3,4)}(q,\omega)$. The main results can be summarized as follows.

(i) The role of spin correlations has been investigated. The differences between the density sum rules and the spin-dependent sum rules become rapidly small by increasing q. The approximation $S^{(3,3)}(q,\omega)=S_I^{(3,3)}(q,\omega)$ is found to be good for typical q's used in neutron-scattering experiments.

(ii) The cross term $S^{(3,4)}(q,\omega)$ gives contributions to the total sum rules of the same order than $S^{(3,3)}(q,\omega)$ in a relevant range of q.[29] A simple qualitative model has been proposed for the cross term, consistent with the microscopic sum rules and in agreement with the quenching of the ^{3}He p-h peak in the experimental spectrum.[6]

(iii) The dynamic structure function in the deep-inelastic limit has been analyzed. The exact sum rules have been compared with the ones from both the incoherent and the impulse approximations. A prediction for $S(q,\omega)$ in the impulse approximation has been given. The evaluation of the mean kinetic energy per ^{3}He particle from the dynamic structure function has also been discussed.

ACKNOWLEDGMENTS

This work was supported in part by DGICYT (Spain) Grant No. PB89-0332, and by INFN, Gruppo Collegato di Trento.

[1]L. D. Landau and I. Pomeranchuk, Dokl. Akad. Nauk. SSSR **59**, 669 (1948).

[2]G. Baym and C. Pethick, in *The Physics of Liquid and Solid Helium,* edited by K. H. Bennemann and J. B. Ketterson (Wiley, New York, 1978), Part II, p. 123.

[3]M. Saarela and E. Krotscheck, in *Recent Progress in Many Body Theories,* edited by T. L. Ainsworth *et al.* (Plenum, New York, 1992), Vol. III, p. 207.

[4]J. Boronat, A. Polls, and A. Fabrocini, J. Low Temp. Phys. (to be published).

[5]R. A. Aziz, V. P. S. Nain, J. S. Carley, W. L. Taylor, and G. T. McConville, J. Chem. Phys. **70**, 4330 (1979).

[6]B. Fåk, K. Guckelsberger, M. Körfer, R. Scherm, and A. J. Dianoux, Phys. Rev. B **41**, 8732 (1990).

[7]P. E. Sokol (private communication).

[8]J. Ruvalds, J. Slinkman, A. K. Rajagopal, and A. Bagchi, Phys. Rev. B **16**, 2047 (1977).

[9]K. S. Pedersen and R. A. Cowley, J. Phys. C **16**, 2671 (1983).

[10]M. Lücke and A. Szprynger, Phys. Rev. B **26**, 1374 (1982); A. Szprynger and M. Lücke, *ibid.* **32**, 4442 (1985).

[11]W. Hsu, D. Pines, and C. H. Aldrich, III, Phys. Rev. B **32**, 7179 (1985).
[12]J. Boronat, A. Polls, and A. Fabrocini, in *Condensed Matter Theories,* edited by V. C. Aguilera-Navarro (Plenum, New York, 1990), Vol. 5, p. 27.
[13]J. Boronat, A. Polls, and A. Fabrocini (unpublished).
[14]S. Stringari, Phys. Rev. B **46**, 2974 (1992).
[15]F. Dalfovo and S. Stringari, Phys. Rev. Lett. **63**, 532 (1989).
[16]C. E. Campbell, J. Low Temp. Phys. **4**, 433 (1971); Hing-Tat Tan, Chia-Wei Woo, and F. Y. Wu, *ibid.* **5**, 261 (1971).
[17]V. F. Sears, J. Phys. C **9**, 409 (1976).
[18]H. R. Glyde and E. C. Svensson, in *Methods of Experimental Physics,* edited by D. L. Price and K. Sköld (Academic, New York, 1987), Vol. 23B, p. 303.
[19]E. Feenberg, in *Theory of Quantum Fluids* (Academic, New York, 1969).
[20]R. D. Puff, Phys. Rev. **137**, A406 (1965).
[21]In pure ^{4}He the multiparticle (or multiphonon) part of $S(q,\omega)$ can be extracted from the experimental spectrum [see, for instance, R. A. Cowley and A. D. B. Woods, Can. J. Phys. **49**, 177 (1971)]. Although the strength of the multiparticle band increases with pressure, the average energies $\hbar\omega_{10}$ and $\hbar\omega_{31}$ are expected to be almost pressure independent.
[22]H. A. Gersch, L. J. Rodriguez, and P. N. Smith, Phys. Rev. A **5**, 1547 (1972).
[23]S. W. Lovesey, *Theory of Neutron Scattering From Condensed Matter* (Oxford University Press, Oxford, 1984); D. L. Price and K. Sköld, in *Methods of Experimental Physics,* edited by K. Sköld and D. L. Price (Academic, New York, 1986), Vol. 23A, p. 1.
[24]T. R. Sosnick, W. M. Snow, R. N. Silver, and P. E. Sokol, Phys. Rev. B **43**, 216 (1991).
[25]P. E. Sokol, Can. J. Phys. **65**, 1393 (1987).
[26]C. Carraro and S. E. Koonin, Phys. Rev. Lett. **65**, 2792 (1990).
[27]M. H. Kalos, M. A. Lee, P. Whitlock, and G. V. Chester, Phys. Rev. B **24**, 115 (1981).
[28]R. M. Panoff and J. Carlson, Phys. Rev. Lett. **62**, 1130 (1989).
[29]A similar conclusion about the non-negligible role of $S^{(3,4)}(q,\omega)$ in the p-h range is also contained in a very recent work by E. Krotscheck and M. Saarela, Phys. Rep. (to be published).